Variance matrix priors for Dirichlet process mixture models with Gaussian kernels.

Wei Jing¹, Michail Papathomas¹ and Silvia Liverani²

¹ School of Mathematics and Statistics, University of St Andrews, UK e-mail: wj4@st-andrews.ac.uk e-mail: M.Papathomas@st-andrews.ac.uk

² School of Mathematical Sciences, Queen Mary University of London, London, UK and The Alan Turing Institute, The British Library, London, UK e-mail: s.liverani@qmul.ac.uk

Abstract: The Dirichlet Process Mixture Model (DPMM) is a Bayesian non-parametric approach widely used for density estimation and clustering. In this manuscript, we study the choice of prior for the variance or precision matrix when Gaussian kernels are adopted. Typically, in the relevant literature, the assessment of mixture models is done by considering observations in a space of only a handful of dimensions. Instead, we are concerned with more realistic problems of higher dimensionality, in a space of up to 20 dimensions. We observe that the choice of prior is increasingly important as the dimensionality of the problem increases. After identifying certain undesirable properties of standard priors in problems of higher dimensionality, we review and implement possible alternative priors. The most promising priors are identified, as well as other factors that affect the convergence of MCMC samplers. Our results show that the choice of prior is critical for deriving reliable posterior inferences. This manuscript offers a thorough overview and comparative investigation into possible priors, with detailed guidelines for their implementation. Although our work focuses on the use of the DPMM in clustering, it is also applicable to density estimation.

Keywords and phrases: Bayesian nonparametrics, clustering.

1. Introduction

The Dirichlet Process Mixture Model (DPMM) is a popular non-parametric Bayesian modelling approach, widely used for density estimation and clustering. In this manuscript, we focus on clustering applications, although the results are also applicable to density estimation. The DPMM allows for model based clustering, where the mixture distribution is the likelihood for each vector observation. For continuous data, the kernel distribution in the mixture likelihood is typically set to be the multivariate Gaussian density. Under the Bayesian framework, when the variance matrix of the Gaussian kernels is unknown, a prior should be specified for it. Due to computational simplicity, the inverse Wishart distribution is often chosen.

Based on our simulation studies, the DPMM struggles to uncover clearly distinct clusters under this choice, even when the dataset consists of just a handful of variables and the normality assumption is correct. Adding hyperpriors

on the parameters of the inverse Wishart distribution does not improve the performance of the model to a satisfactory degree, as we demonstrate in Section 4

In this manuscript, we consider problems in a space of up to 20 dimensions. This is a higher dimensionality than usually tested in simulation studies, relevant to more realistic problems. It can be viewed as high dimensionality in particular within the context of clustering, when unknown covariance matrices are to be estimated for a selection of clusters, some potentially of small size.

Some standard approaches for tackling the problem of dimensionality, listed in Chandra et al. (2020), involve strong assumptions on the structure of the covariance matrix. One assumption, for instance, is that variables are conditionally independent given the cluster allocation. This presumes clusters of specific shape and orientation, and the DPMM can perform badly when this assumption is violated; see also Section 4 and the Supplemental material Section S5.1.

We observe that the choice of prior for the variance matrix of the Gaussian kernel is increasingly important as the dimensionality as well as the number of target clusters increases. Using simulated and real data, we demonstrate that a sparsity inducing prior is the most promising one, in terms of effecting MCMC convergence and identifying true clusters.

When the DPMM model is adopted, the number of components in the mixture is set to be infinite. The likelihood for each data point X_i in \mathbb{R}^J is,

$$X_i | \boldsymbol{\psi}, \boldsymbol{\Theta} \sim \sum_{c=1}^{\infty} \psi_c f(X_i | \boldsymbol{\Theta}_c),$$
 (1.1)

where $X_i = [X_{i,1}, X_{i,1}, ..., X_{i,J}]^T$ is the data vector for subject i, after observing J variables. Here, $f(X_i|\Theta_c)$ represents a family of distributions with cluster specific parameters Θ_c for component c. Also, ψ_c denotes the latent probability with which X_i belongs to component c, with $\sum_{c=1}^{\infty} \psi_c = 1$. To simplify the likelihood and subsequent computations, an auxiliary vector $\mathbf{Z} = [Z_1, Z_2, ..., Z_n]$ is often introduced. Conditionally on \mathbf{Z} , the infinite mixture likelihood becomes,

$$X_i|Z_i, \mathbf{\Theta} \sim f(X_i|\mathbf{\Theta}_{Z_i}).$$
 (1.2)

Conditionally on ψ , the probability mass function of Z_i is,

$$p(Z_i = c|\boldsymbol{\psi}) = \psi_c$$

The core part of the DPMM is the Dirichlet process (DP). Denote by $\tilde{\mathbf{\Theta}} = (\tilde{\mathbf{\Theta}}_1, ..., \tilde{\mathbf{\Theta}}_n)$, the vector of cluster specific parameters for subjects i = 1, ..., n. Elements of this vector can be identical, so that if subjects i and i' belong to cluster c, then $\tilde{\mathbf{\Theta}}_i = \tilde{\mathbf{\Theta}}_{i'} = \mathbf{\Theta}_c$. The DP can be represented with the stick-

breaking construction Sethuraman (1994) given below.

$$G = \sum_{c=1}^{\infty} \psi_c \delta_{\Theta_c}$$

$$\psi_c = V_c \prod_{l < c} (1 - V_l), \quad \psi_1 = V_1$$

$$V_c | \alpha \sim Beta(1, \alpha)$$

$$\Theta_c | G_0 \sim G_0,$$

$$(1.3)$$

where G_0 denotes the base distribution defined on the parameter space of Θ_c and α is the concentration parameter. As the realization of the DP is almost surely discrete (Blackwell, 1973), the DPMM is introduced so that the distribution of the X_i can be absolutely continuous (Lo, 1984), namely

$$X_i | \tilde{\mathbf{\Theta}}_i \sim f(X_i | \tilde{\mathbf{\Theta}}_i)$$

 $\tilde{\mathbf{\Theta}}_i | G \sim G$ (1.4)
 $G | G_0, \alpha \sim DP(G_0, \alpha),$

where the $\tilde{\Theta}$ parameters are drawn using (1.3).

Based on (1.2), (1.3) and (1.4), the joint distribution of the data and parameters becomes

$$p(X_i, \mathbf{\Theta}, \boldsymbol{\psi} | \alpha, G_0, Z_i) = f(X_i | \mathbf{\Theta}_{Z_i}) p(\mathbf{\Theta}) p(\boldsymbol{\psi})$$

$$= f(X_i | \mathbf{\Theta}_{Z_i}) \Big\{ \prod_{c=1}^{\infty} p(\mathbf{\Theta}_c) p(\psi_c) \Big\}.$$
(1.5)

For datasets that contain only continuous variables, the typical choice for the component distribution is the multivariate normal density, namely,

$$f(X_i|\mathbf{\Theta}_{Z_i}) = (2\pi)^{-\frac{J}{2}} |\Sigma_{Z_i}|^{-\frac{1}{2}} \exp\left\{-\frac{1}{2}(X_i - \mu_{Z_i})^T \Sigma_{Z_i}^{-1}(X_i - \mu_{Z_i})\right\}, \quad (1.6)$$

where μ_{Z_i} and Σ_{Z_i} are the mean vector and the variance-covariance matrix for cluster Z_i respectively. In this case, $\Theta_{Z_i} = (\mu_{Z_i}, \Sigma_{Z_i})$. One commonly used setting for the base distribution G_0 is,

$$G_0 \equiv N_J(\mu_c; \mu_0, \Sigma_0) \times InvWishart_J(\Sigma_c; R_0, \kappa_0), \tag{1.7}$$

where N_J denotes the multivariate normal distribution of dimension J (with mean μ_0 and covariance matrix Σ_0); $InvWishart_J$ represents the Inverse Wishart distribution (IW) of dimension J (with mean matrix R_0 and scale parameter κ_0). Note that μ_c and Σ_c are independent a priori.

Despite being commonly employed as the prior for a variance-covariance matrix, the Inverse Wishart distribution has received a great amount of criticism in the literature. Gelman (2006) stated that the IW allocates little mass for

Cluster No.	μ_c^{true}	Var_c^{true}	$ ho_c^{true}$	n_c
1	(5, 35, 75, 5, 5, 5)	1	0	100
2	(35, 5, 5, 5, 5, 5)	1	0	100
3	(5, 75, 5, 5, 5, 35)	1	0	100
4	(5, 5, 35, 5, 5, 75)	1	0	100
5	(35, 75, 35, 5, 5, 5)	1	0	100

Table 2

Simulated data II with J=20. rep(a,b) is a vector of length b with repeated elements a. The Var_c^{true} and ρ_c^{true} columns show the identical diagonal elements, and identical correlations in Σ_c^{true} respectively.

Cluster No.	μ_c^{true}	Var_c^{true}	ρ_c^{true}	n_c
1	(rep(3,5), rep(32,5), rep(35,5), rep(72,5))	5	0.2	200
2	(rep(32,5), rep(5,5), rep(5,5), rep(35,5))	5	0.5	200
3	(rep(25,5), rep(15,5), rep(32,5) rep(3,5))	5	0.3	200
4	(rep(15,5), rep(75,5), rep(8,5), rep(75,5))	5	0.1	200
5	(rep(8,5), rep(6,5), rep(25,5), rep(5,5))	5	0.7	200

variances in the region near zero. O'Hagan (1994) pointed out that the IW uses only one degree of freedom (κ_0) to model the variability and dependence between all the parameters in the matrix. Consequently, a great amount of dependency among the entries of correlations and variances is introduced. More specifically, the larger the variances, the larger the correlations in absolute value (Tokuda et al., 2011). Lastly, the IW is sensitive to the choice of the hyperparameter values (Hennig et al., 2015).

We illustrate the problem of using the IW in the context of the DPMM with two simulation examples, with specifications given in Table 1 (well-separated clusters, with small cluster-specific variances within Σ_c^{true} , and large sample size in relation to the number of model parameters) and Table 2 (clusters are closer, with larger cluster-specific variances and small sample size). Five clusters are simulated from the multivariate normal distribution. In the Supplementary material, Section S7, we include reduced dimensionality plots of the generated true clusters for one dataset for each simulation scenario.

We generate 20 datasets for each scenario, and adopt the IW prior using the R package PReMiuM (Liverani et al., 2015). We choose a burn-in period of 10,000 iterations followed by 6,000 iterations. Posterior samples for the allocation vector \mathbf{Z} show that the induced partition becomes stable after this burn-in period. Under both scenarios true clusters are merged, with notably different clustering results for datasets with the same underlying structure. Figure 1 (for simulated data I) shows the bar plot of the estimated number of clusters for the 20 datasets, generated from post-processing the MCMC output (Molitor et al., 2010) for each dataset. It also shows posterior density plots of α for each of the 20 datasets. Figure 2 shows corresponding results for simulation data II. Note that similar results are also obtained by the R package DPackage (Jara et al., 2011).

When true clusters are combined, posterior variances within some Σ_c are larger than the truth. This can be explored in more detail when the IW is utilised; see the Supplemental material, Section S1 for details. One way to tackle the problem is to set R_0 in (1.7) to be small, for example, the identity matrix. Although this is effective for Simulation I, it is not for Simulation II or real datasets we have analysed, as the IW is sensitive to the specification of the hyperparameter values. Celeux et al. (2018) proposed a strategy for choosing the value of R_0 in the context of sparse finite mixture model (Malsiner-Walli et al., 2016). The setting worked well most times, with 3 true clusters and diagonal within-cluster covariance matrices. However, the authors also mentioned that when the number of subjects is small, true clusters can be combined. As in (1.7) κ_0 and R_0 are fixed, one can instead choose to place hyperpriors on those hyperparameters. This can improve the performance for some analyses, but does not provide with a satisfactory solution in general. This is discussed in detail in Section 4.

Finally, the MCMC sampler initialisation plays a role in the performance of the DPMM, since typically there is a discrepancy between the overall covariance matrix and the within-cluster covariance matrices; see Supplemental material, Section S2. A more detailed discussion about initialization is provided in Section 5.

The challenges to the DPMM caused by the estimation of Σ_c are not obvious when one simulates or analyses only a small number of continuous variables (say J < 4) and the number of target clusters are only, say, 2 or 3, as is usually the case for simulation studies that assess DPMM models. As J and the number of target clusters increases, the problem becomes more pronounced since the number of parameters in each Σ_c increases quadratically.

In the next section, we review alternative prior specifications for the variance matrix and discuss their implementation. In Section 3, we discuss the prior specification of the mean vector in the Gaussian kernel for the DPMM. In Section 4, we compare the performance of different priors with simulation examples. In Section 5, we consider specifications that influence the performance of the DPMM not discussed before. Section 6 shows a real data comparative analysis. Section 7 summarises our findings on the best performing prior specification, and provides future research directions.

2. Alternative priors to the Inverse Wishart

In this Section, we introduce a variety of priors we incorporated into the DPMM framework, with details on their implementation (e.g. full conditional distributions) provided in the Supplemental material, Section S5. This was done within the R package PReMiuM (Liverani et al., 2015) which accommodates continuous and categorical observations; see also Molitor et al. (2010). It employs the conditional samplers based on the stick-breaking construction in (1.3). In particular, we modified a version of the slice sampler by Walker (2007), used as the default sampler in PReMiuM. For details of this default sampler see the Supplemental material Section S3 and Liverani et al. (2015).

2.1. The hierarchical Inverse Wishart prior (HIW)

This is an extension to the IW, with hyperpriors on R_0 and κ_0 so that they can be estimated from the data. The simplest hyperprior for R_0 is the Wishart prior, namely,

$$\Sigma | R_0, \kappa_0 \sim InvWishart_J(R_0, \kappa_0),$$

$$R_0 | R_1^{-1}, \kappa_1 \sim Wishart_J(R_0; R_1^{-1}, \kappa_1).$$
(2.1)

The formulation in (2.1) has already been applied in the DPMM literature; see Görür and Rasmussen (2010) for instance. It is computationally fast because no Metropolis-Hastings steps are involved and R_0 is updated all at once. Within the context of the DPMM, the prior of Σ_c in (2.1) can be written as

$$\Sigma_{c}|R_{0}, \kappa_{0} \sim InvWishart_{J}(\Sigma_{c}; R_{0}, \kappa_{0}),$$

$$R_{0}|R_{1}^{-1}, \kappa_{1} \sim Wishart_{J}(R_{0}; R_{1}^{-1}, \kappa_{1}),$$

$$\kappa_{0} - J|\alpha_{\kappa_{0}}, \beta_{\kappa_{0}} \sim InvGamma(\kappa_{0} - J; \alpha_{\kappa_{0}}, \beta_{\kappa_{0}}),$$

$$(2.2)$$

where InvGamma denotes the Inverse Gamma distribution. Note that $\kappa_0 > J$. We refer to the prior in (2.2) as HIW1. Hyperparameter values are set to be,

$$R_1 = I_J, \quad \alpha_{\kappa_0} = 1/2, \quad \beta_{\kappa_0} = \frac{J}{2}, \quad \kappa_1 = J + 2,$$

which results in relatively small mean within-cluster variances a priori. Huang and Wand (2013) suggested another conditional conjugate prior for Σ as follows,

$$\Sigma_c|\epsilon_0, \delta_1, ..., \delta_J \sim InvWishart_J(\Sigma_c; 2\epsilon_0 diag(1/\delta_1, ..., 1/\delta_J); \epsilon_0 + J - 1),$$

$$\delta_j|g_j \sim InvGamma(\delta_j; 1/2, 1/g_j^2).$$
(2.3)

Huang and Wand (2013) proved that the standard deviation in the covariance matrix follows a Half-t distribution, which is recommended by Gelman [11].

For j = 1, ..., J the prior of Σ_c in (2.3) can be written as

$$\Sigma_{c}|\epsilon_{0}, \delta_{j,j=1,...,J} \sim InvWishart_{J}\left(\Sigma_{c}; 2\epsilon_{0}diag\left(\frac{1}{\delta_{1}}, ..., \frac{1}{\delta_{J}}\right), \epsilon_{0} + J - 1\right),$$

$$\delta_{j}|\alpha_{\delta}, g_{j} \sim InvGamma(\delta_{j}; \alpha_{\delta}, g_{j}),$$

$$(\epsilon_{0} - 1)|\alpha_{\epsilon_{0}}, \beta_{\epsilon_{0}} \sim InvGamma(\epsilon_{0} - 1; \alpha_{\epsilon_{0}}, \beta_{\epsilon_{0}}).$$

$$(2.4)$$

We refer to the prior in (2.4) as HIW2. The hyperparameter values are set to be.

$$g_j = \frac{J * 20.0}{range(\mathbf{X}_j) * range(\mathbf{X}_j)}, \quad \alpha_{\delta} = 0.2, \quad \beta_{\epsilon_0} = \frac{J}{2}, \quad \alpha_{\epsilon_0} = 0.5,$$

which also results in relatively small mean within-cluster variances a priori.

2.2. The separation prior

This construction relies on the idea of decomposing the covariance matrix to variance and correlation matrices (Barnard et al., 2000). Specifically,

$$\Sigma = SRS, \tag{2.5}$$

where $S = \{s_{j,j}\}$ is a diagonal matrix with the standard deviation of each variable as diagonal elements and $R = \{r_{i,j}\}$ is a correlation matrix. Prior distributions can be specified for S and R, so that they are independent or dependent a priori. We refer to priors whose specification is based on (2.5) as separation priors.

Setting a prior for R that allows for efficient sampling from its full conditional distribution is not straightforward. Barnard et al. (2000) suggested two priors. Firstly,

$$p_R \propto |R|^{\frac{J^2 - J - 2}{2}} (\prod_{j=1}^{J} |R_{jj}|)^{-\frac{J+1}{2}},$$
 (2.6)

where |A| denotes the determinant of matrix A, and R_{jj} represents the jth principle submatrix of R. The prior in (2.6) results in a uniform prior on each correlation element $r_{i,j}$. The second prior is a joint uniform prior on R^J , namely,

$$p_R \propto 1.$$
 (2.7)

Updating R element by element is suggested in Barnard et al. (2000). Keeping R positive definite is computationally expensive as it involves solving a quadratic equation before updating each $r_{i,j}$. O'Malley and Zaslavsky (2008) proposed an Inverse Wishart prior for R, which is not restricted to be a correlation matrix any more. The advantage of this setting is the sampling convenience gained by using the conditional conjugate Inverse Wishart distribution. However, variances and correlations in Σ_c can no longer be independent a priori. We adopt a similar specification to O'Malley and Zaslavsky (2008) as shown below.

$$R_{c}|R_{R}, \kappa_{R} \sim InvWishart_{J}(R_{c}; R_{R}^{-1}, \kappa_{R}),$$

$$(\kappa_{R} - J)|\alpha_{\kappa_{R}}, \beta_{\kappa_{R}} \sim InvGamma(\kappa_{R} - J; \alpha_{\kappa_{R}}, \beta_{\kappa_{R}}),$$

$$s_{c,j}|\alpha_{s}, \beta_{sj} \sim InvGamma(s_{c,j}; \alpha_{s}, \beta_{sj}),$$

$$\beta_{sj}|\alpha_{0}, \beta_{0j} \sim Gamma(\beta_{sj}; \alpha_{0}, \beta_{0j}),$$

$$\Sigma_{c} = S_{c}R_{c}S_{c},$$

$$(2.8)$$

where $S_c = \{s_{c,j}\}$ is a diagonal matrix for cluster c and $R_c = \{r_{c,i,j}\}$ is a dense matrix for cluster c. Note that if no constraint is set on R_c , matrices S_c and R_c are not identifiable. However, when the focus is on Σ_c , this may not be of concern. Also, notice that a hyperprior is placed on β_{sj} which is similar to the setting in Richardson and Green (1997). Hyperparameter values are listed

below.

$$R_R = I_J, \quad \alpha_{\kappa_R} = 1/2, \quad \beta_{\kappa_R} = \frac{J}{2},$$

 $\alpha_s = 2, \quad \alpha_0 = 0.2, \quad \beta_{0,j} = \frac{10}{range(X_j)^2}.$

This results in relatively small mean within-cluster variances a priori. Note that under the framework in (2.5), another prior available for matrix R is the LKJ (Lewandowski-Kurowicka-Joe) prior (Lewandowski et al., 2009), with Hamiltonian Markov Chain Monte Carlo (HMCMC) typically used to sample from the posterior. We did not adopt this specification for reasons of computational efficiency.

2.3. The log prior

Another prior specification for the covariance matrix Σ relies on the log transformation $A = \log(\Sigma)$, and the spectral decomposition $\Sigma = EDE^T$. Here, D is a diagonal matrix with the eigenvalues of Σ as diagonal elements and E is an orthonormal matrix. The columns of E are normalized eigenvectors, and correspond to the eigenvalues of D. Based on the above,

$$A = E \log(D) E^T$$
,

where $\log(D)$ is a diagonal matrix with the logarithm of the eigenvalues of Σ as its diagonal elements. When A is sampled as a symmetric matrix, $\exp(A) = \Sigma$ is positive definite. This specification (referred to as the log prior) was first considered by Leonard and Hsu (1992), who represented A as a vector,

$$\mathbf{a} = (a_{1.1}, a_{2.2}, ..., a_{J.J}; a_{1.2}, ..., a_{J-1.J}; ...; a_{1.J-1}, a_{2.J}; a_{1.J}).$$

A uniform prior, $a \propto 1$, or a multivariate normal prior can be placed on a. We adopt the multivariate normal prior as it is relatively flexible and the elements of $\log(\Sigma)$ can be sampled all at once. In the context of the DPMM, using the subscript c to denote cluster labels,

$$\boldsymbol{a}_c | \mu_{\boldsymbol{a}}, \Sigma_{\boldsymbol{a}} \sim N_q(\boldsymbol{a}_c; \mu_{\boldsymbol{a}}, \Sigma_{\boldsymbol{a}}).$$
 (2.9)

Leonard and Hsu Leonard and Hsu (1992) utilize the Taylor series approximation for the Normal likelihood,

$$\prod_{i=1}^{n_c} f(X_i | \boldsymbol{Z}, \mu_c, \boldsymbol{a}_c) \simeq (2\pi)^{-\frac{n_c}{2}} e^{-Jn_c} |S_c^*|^{-\frac{n_c}{2}} \exp\left\{-\frac{1}{2} (\boldsymbol{a}_c - \boldsymbol{\lambda}_c)^T Q_c (\boldsymbol{a}_c - \boldsymbol{\lambda}_c)\right\},$$
(2.10)

where λ_c is the mean vector, Q_c is the precision matrix and $S_c^* = \frac{1}{n_c} \sum_{c} (X_i - \mu_c)(X_i - \mu_c)^T$. The details of how to compute λ_c and Q_c are given in the Supplemental material, Section S5.

In this conjugate setting, the posterior for a_c is approximately Normal. In the context of DPMM, we use Metropolis-Hastings MCMC to sample from the full conditional distribution of Σ_c . To better explore the sample space of Σ_c , we set the multivariate t distribution as the proposal, which can also serve as the importance function for the importance sampling algorithm in Leonard and Hsu (1992).

Because the multivariate normal prior for a_c is already quite flexible, we assigned fixed values to the hyperparameters $\mu_{\boldsymbol{a}}$ and $\Sigma_{\boldsymbol{a}}$. We set $\mu_{\boldsymbol{a}} = (-1, \dots, -1, 0, \dots, 0)$, where the first J elements are non-zero. The specification of -1 makes the variances in Σ_c relatively small. We also set $\Sigma_{\boldsymbol{a}} = diag(3, \dots, 3, 1, \dots, 1)$, with the first J elements in the diagonal equal to 3.

The advantage of using the log transformation is that it is relatively easy to implement and the sampling method allows to update the vector \mathbf{a}_c all at once. However, whether the sampler for \mathbf{a}_c can mix well depends on the quality of the approximation in (2.10). In addition, the calculation of matrix Q_c is non-trivial especially for large J.

2.4. The sparse prior

For the estimation of a sparse precision or covariance matrix, the graphical and adaptive graphical lasso within the frequentist framework [Yuan and Lin (2007); Friedman et al. (2008); Fan et al. (2009)] are equivalent to placing the Laplace prior on the off-diagonal elements and the exponential prior on the diagonal elements of the precision matrix [Wang (2012); Khondker et al. (2013)]. Specifically,

$$X_{i}|T \sim N_{J}(\mathbf{0}, T^{-1}),$$

$$p(T|M_{0}) = C_{0}^{-1} \prod_{i < j} \left\{ Laplace(T_{ij}|0, 1/m_{0,ij}) \right\} \prod_{i} \left\{ Exp(T_{ii}|m_{0,ii}/2) \right\}, \ T \in P^{+},$$

$$(2.11)$$

where T denotes the precision matrix and P^+ is the set of all positive definite matrices. C_0^{-1} is a normalizing constant. The hyperparameters $m_{0,ij}$ control the amount of shrinkage of T_{ij} towards zero and can be arranged into matrix $M_0 = \{m_{0,ij}\}$. MCMC algorithms for sampling from the resulting posterior are given by Wang (2012) and Khondker et al. (2013).

The construction in (2.11) can not result in exact zero posterior estimates of T_{ij} . To avoid a thresholding approach, a spike-and-slab [Mitchell and Beauchamp (1988); George and McCulloch (1993, 1997)] type prior puts a point mass at $T_{ij} = 0$ and a continuous distribution when $T_{ij} \neq 0$, as in Banerjee and Ghosal (2013). However, posterior computation becomes cumbersome and Banerjee and Ghosal (2013) utilized the Laplace approximation. For this reason, we focus on the prior in (2.11). We implement the sampler proposed by Wang (2012) as it does not require Metropolis-Hastings steps.

The Laplace distribution can be represented as a scale mixture of Normals.

This suggests that the prior for T can be written as,

$$p(T|M_0, M_1) = C_1^{-1} \prod_{i < j} \left\{ N(T_{ij}|0, m_{1,ij}) \right\} \prod_i \left\{ Exp(T_{ii}|m_{0,ii}/2) \right\}, \ T \in P^+,$$
(2.12)

where $m_{1,ij}$ are auxiliary variables that can be arranged into a matrix $M_1 = \{m_{1,ij}\}$ with diagonal elements zero. C_1^{-1} is another normalizing constant. Wang (2012) constructed the prior of M_1 as,

$$P(M_1|M_0) \propto C_1 \prod_{i < j} Exp(m_{1,ij}|m_{0,ij}^2/2).$$
 (2.13)

After integrating out $m_{1,ij}$, T follows the Laplace distribution given in (2.11). Therefore, the specification of the sparse prior in the context of the DPMM can be provided as,

$$p(T_c|M_0, M_{1,c}) = C_{1,c}^{-1} \prod_{i < j} \left\{ N(T_{c,ij}|0, m_{1,c,ij}) \right\} \prod_i \left\{ Exp(T_{c,ii}|m_{0,ii}/2) \right\}, \ T_c \in P^+,$$

$$P(M_{1,c}|M_0) \propto C_{1,c} \prod_{i < j} Exp(m_{1,c,ij}|m_{0,ij}^2/2).$$
(2.14)

Here, $M_{1,c}$ is the cluster specific matrix that corresponds to M_1 . The prior contains the intractable normalizing constant $C_{1,c}$ $\{c \in P\}$, but this cancels out when sampling from the joint prior,

$$P(T_c, M_{1,c}|M_0)$$

$$\propto \prod_{i < j} \left\{ N(T_{c,ij}|0, m_{1,c,ij}) Exp(m_{1,c,ij}|m_{0,ij}^2/2) \right\} \prod_i \left\{ Exp(T_{c,ii}|m_{0,ii}/2) \right\}, \ T_c \in P^+.$$

It is required to sample from this prior when sampling for the parameters of empty clusters. (For non-empty clusters, in the full conditional distribution of $M_{1,c}$, the normalizing constant $C_{1,c}$ also cancels out.) To increase the efficiency of the MCMC sampler, we set what we argue are preferred initial values for T_c and $M_{1,c}$. Additional details are provided in the Supplementary material, Section S5.6.

Figure 3 shows empirical prior distributions for the correlations, and empirical bivariate density plots for the variances for different M_0 . These and other empirical results not shown here indicate that smaller values of diagonal elements $m_{0,ii}$ correspond to smaller variances in Σ_c and a prior density for the correlations that is more concentrated around zero. This is also the effect of larger off-diagonal values of $m_{0,ij}$.

Within the context of the DPMM, we observed that values of M_0 that imply correlations very close to zero are restrictive and clustering results are unsatisfactory. M_0 values that lead to a less spiky density for the correlations result in much better performance. Note that the prior distribution of the correlations should not be too flat. It should still imply a higher probability of generating

small correlations, but should allow for larger correlations in absolute value in the tail. The prior range of the within-cluster variances is also important. When variances are too small a priori, the final clustering can contain many small clusters; whereas, when variances are too large, the final clustering can combine true clusters. We suggest tuning the values in M_0 as follows: plot the dataset using some dimension reduction technique (as discussed in Section 4 and the supplementary material, Section S7) and calculate the sample variances from the the whole dataset. If there is no clear separation of groups of data points (which is normally the case for real datasets), then set the value of M_0 such that the expected within-cluster variances are concentrated just below the largest overall variances. If there is clear separation of data clusters, set the value of M_0 so that the within-cluster expected variances are concentrated at approximately half of the largest overall variance. In both cases, set the value of M_0 such that the prior distributions for the correlations are relatively uninformative. For this, we have found that a reasonable setting can be $\frac{m_{0,ij}}{m_{0,ii}} = 3$. For the simulated and real datasets analysed in this manuscript, we set $m_{0,ii} = 10$ and $m_{0,ij} = 30$, for

In the setting given in (2.11), all of the elements in M_0 are fixed. In the context of the DPMM, one can also place a hyperprior on M_0 . The difficulty in doing so lies in the derivation of the posterior of M_0 . Wang (2012) proves that only when $m_{0,ij}$ and $m_{0,ii}$ are all equal, C_0^{-1} is not a function of M_0 . Therefore, to set hyperpriors for M_0 , we let M_0 be component specific, namely

$$p(T_{c}|M_{0,c}) = C_{0,c}^{-1} \prod_{i < j} \left\{ Laplace(T_{c,ij}|0, 1/m_{0,c,ij}) \right\} \prod_{i} \left\{ Exp(T_{c,ii}|m_{0,c,ii}/2) \right\},$$

$$p(M_{0,c}) \propto C_{0,c} \prod_{i < j} \left\{ Gamma(m_{0,c,ij}|\alpha_{m_0}, \beta_{m_0}) \right\} \prod_{i} \left\{ Gamma(m_{0,c,ii}|\alpha_{m}, \beta_{m}) \right\},$$

$$(2.15)$$

so that the posterior conditional distributions of $M_{0,c}$ do not involve $C_{0,c}$. However, empirical results showed that the fixed M_0 setting generates better clustering results.

For different choices of $\{\alpha_m, \beta_m, \alpha_{m_0}, \beta_{m_0}\}$ we observed that, as the hyperprior placed on $M_{0,c}$ is cluster specific, the prior for T_c after integrating $M_{0,c}$ out is less flexible than the prior of T_c based on M_0 . In addition, the model includes a large number of parameters after making M_0 cluster specific, which slows down computational speed. Therefore, we choose the specification with a fixed M_0 and refer to it as the sparse prior in the rest of this manuscript.

3. The base distribution of μ_c

Besides the base distribution of Σ_c , it is also beneficial to place hyperpriors on the parameters μ_0 and Σ_0 of the base distribution for μ_c in (1.7). Since μ_c and Σ_c are independent a priori, adding hyperpriors on μ_0 and Σ_0 does not affect the algebraic form of the conditional posterior distributions for Σ_c given in Section 2. One choice of hyperpriors for μ_0 and Σ_0 is given below.

$$\mu_{c}|\mu_{0}, \Sigma_{0} \sim N_{J}(\mu_{c}; \mu_{0}, \Sigma_{0}),
\mu_{0}|\mu_{00}, \Sigma_{00} \sim N_{J}(\mu_{0}; \mu_{00}, \Sigma_{00}),
\Sigma_{0}|R_{00}^{-1}, \kappa_{00} \sim InvWishart_{J}(\Sigma_{0}; R_{00}^{-1}, \kappa_{00}).$$
(3.1)

The values of the hyperparameters $\{\mu_{00}, \Sigma_{00}, R_{00}^{-1}, \kappa_{00}\}$ are set to be

$$\mu_{00} = \frac{1}{n} \sum_{i=1}^{n} X_i, \ \Sigma_{00} = Diag(range(X_1)^2, range(X_2)^2, ..., range(X_J)^2),$$

$$R_{00} = \Sigma_{00}^{-1}, \ \kappa_{00} = J + 2,$$

which results in reasonably vague priors for μ_0 and Σ_0 .

The specification in (3.1) is conditional conjugate, as the conditional posterior distributions of μ_0 and Σ_0 are of standard form; see Supplemental material, Section S6.

Empirical results from implementing the priors in (3.1) showed that placing a hyperprior on μ_0 can improve the performance of the DPMM. Simulation studies did not show that adding a hyperprior on Σ_0 improves clustering results. Therefore, we only implement the hyperprior for μ_0 in (3.1) in all subsequent analyses.

4. Comparison of different priors using simulated data

In this Section, we compare the performance of the priors discussed in Section 2. We add to the comparisons the setting where within-cluster independence is assumed for the observed variables (see Supplemental material Section S5.1). An Inverse Gamma prior is specified for the variance parameters. We refer to this settings as the independent prior. The adjusted Rand index is used to compare the different priors. Assuming the cluster allocation vector \boldsymbol{Z} is of length n, the Rand index is defined as,

$$Rand\ index = \frac{TP + TN}{\binom{n}{2}},\tag{4.1}$$

where TP denotes the number of pairs of observations correctly allocated to the same cluster. TN denotes the number of pairs correctly allocated to different clusters. Hubert and Arabie (1985) proposed the adjusted Rand index, which is defined as follows

$$\frac{index-expected\ index}{maximum\ index-expected\ index}. \tag{4.2}$$

We adopt the adjusted Rand index for our comparative study, recommended by Milligan and Cooper (1986) in their review.

Observations are generated using multivariate normal distributions with cluster specific means and covariance matrices. Two simulation settings for the

within-cluster correlation matrices are considered. In the first dense setting, all correlations are non-zero. Within a matrix, all ρ_c^{true} correlations are identical. In the second sparse setting, within-cluster correlation matrices are block diagonal. Variables are highly correlated within each block and independent between blocks. Non-zero correlations within a matrix are identical. Two simulation scenarios are considered within each setting. One with larger within-cluster variances where the clusters are not well separated, and another with smaller within-cluster variances where, although the clusters are more separated, the simulations are still challenging.

20 datasets are generated for each scenario and setting combination. Burn-in consists of 10,000 iterations, with 6,000 additional iterations. Posterior allocation samples were stable after the burn-in period. We compare the performance of the priors in terms of: (a) the number and profile of clusters in the 'best-representation' clustering obtained from the post-processing of the MCMC output (Molitor et al., 2010); (b) the adjusted Rand index; (c) computing time.

4.1. Simulations with dense within-cluster covariance matrices

The two dense simulation settings are given in Tables 3 and 4. Five clusters are simulated. The sample size for each cluster ($n_c = 200$) is relatively small compared to the number of cluster-specific parameters for J = 20. More than 80% of the variability is explained by the first three Principle Components (PCs); see Supplemental material, Section S8. Those PCs are used to visualize the clusters. Reduced space plots for one representative simulated dataset III and another dataset IV are given in Figure 4. Simulated data III (Table 3) have smaller variances, which translates to a stronger clustering signal. Clusters in simulated data IV (Table 4) are closer and the signal is less strong. Plots of the overall covariance matrices are given in the Supplemental material, Section S8.

Table 3 Simulated data III specifications. J = 20. rep(a,b) represents a vector of length b with repeated elements a.

Cluster No.	μ_c^{true}	$\operatorname{Var}_{c}^{true}$	$ ho_c^{true}$	n_c
1	(rep(3,5), rep(12,5), rep(18,5), rep(12,5))	3	0.2	200
2	(rep(12,5), rep(18,5), rep(3,5), rep(18,5))	3	0.5	200
3	(rep(18,5), rep(18,5), rep(12,5), rep(8,5))	3	0.3	200
4	(rep(18,5), rep(3,5), rep(8,5), rep(3,5))	3	0.1	200
5	(rep(8,5), rep(8,5), rep(12,5), rep(3,5))	3	0.7	200

Cluster No.	μ_c^{true}	Var_c^{true}	$ ho_c^{true}$	n_c
1	(rep(3,5), rep(12,5), rep(18,5), rep(12,5))	9	0.2	200
2	(rep(12,5), rep(18,5), rep(3,5), rep(18,5))	9	0.5	200
3	(rep(18,5), rep(18,5), rep(12,5)rep(8,5))	9	0.3	200
4	(rep(18,5), rep(3,5), rep(8,5), rep(3,5))	9	0.1	200
5	(rep(8,5), rep(8,5), rep(12,5), rep(3,5))	9	0.7	200

Bar plots of the number of clusters recognised for each of the 7 priors are shown in Figures 5 and 6. More important for assessing performance is the profile of the clusters, in terms of containing observations that were truly generated by the same mixture component. Figure 7 shows boxplots of the adjusted Rand indices for different priors.

The number of identified clusters when the IW and HIW2 priors are employed is usually lower than the true number of clusters since true clusters are combined together. This leads to unsatisfactory performance in terms of adjusted Rand index. The independent prior consistently recognizes more clusters than the truth, as it splits true clusters into clusters of substantial size. This is illustrated in Figure 8, where representative partitions corresponding to the HIW1, sparse and independent priors are shown, when all three priors identify 9 clusters for simulated data IV.

The log prior is the worst performer. The number of identified clusters can either be small or very large (beyond 20 clusters). The adjusted Rand indices for both data III and IV are volatile and low in value. The bad performance is partly due to the poor approximation of the likelihood in (2.10). The approximation assumes that μ_c is known and, furthermore, only uses up to the quadratic term in the Taylor expansion. This leads to notably bad performance when the dimensionality increases in the context of the DPMM.

Overall, the sparse prior is the best performer in terms of the adjusted Rand index and the profile of the generated clusters. For simulated data III, its Rand indices always equal one and for simulated data IV they are always very close to one. The Rand indices for the separation prior are usually close to one, except for two outliers for simulated data IV. Such low outliers in the box-plot typically occur when true clusters are combined together. There is more variability in the performance of the HIW1 prior compared to the sparse and separation priors. The superfluous clusters generated by the HIW1 are not clearly defined; see Figure 8 for instance. The sparse prior also identifies superfluous clusters, but its behaviour is different. For example, when the sparse prior identifies 9 clusters, superfluous clusters only contain one or two subjects per cluster; see Figure 8. Thus, the posterior partition is similar to the true partition with adjusted Rand index close to one.

It is worth noting that the HIW2 performs worse than the HIW1 possibly because when R_0 is restricted to diagonal, some information from the data can not be incorporated into R_0 . This can be seen by comparing the conditional posteriors (Supplemental material, Section S5), where R_0 is updated using all the information in T_c (for $c \in A$) but δ_j is updated using only the information in the diagonal of T_c , for j = 1, ..., J.

Figure 9 displays the box plot of run-times for each simulated dataset. The log prior is much slower than the others because of the complexity in calculating the precision matrix Q_c of a_c , which is of order $O(J^4)$. Therefore, as J increases, it becomes impractical to use the log prior, not to mention its poor performance. The separation prior is the second slowest because the elements in T_{Sc} are updated element by element using Metropolis-Hastings. Although the time required by the sparse prior is about 2 to 3 times the time required by

HIW1, this still allows for the implementation of the sparse prior in practice. The IW is usually the quickest since its sampler is the simplest. The HIW1 and HIW2 priors are only slightly slower than the IW.

In the Supplemental material, Section S8, plots of the posterior distributions of α , for the different set-ups and datasets are shown. As the value of α is closely related to the number of clusters identified, the bandwidth of the posteriors is closely associated with the results in Figures 5 and 6.

4.2. Simulations with sparse within-cluster covariance matrices

The specifications for the two sparse simulation scenarios are given in Tables 5 (data V) and 6 (data VI). Correlation matrices are block diagonal with 5 blocks. Simulated data V are generated with smaller variances compared to simulated data VI, and thus carry a stronger clustering signal.

In the Supplemental material, Section S9, visualisation plots for the generated clusters are presented. It is shown that both specifications generate challenging data sets, with the clusters being considerably close for datasets VI. In the same section, we also present two Figures that display the number of clusters recognized for each prior for simulated data V and VI.

Boxplots of the adjusted Rand indices for each prior are shown in Figure 10. The log and HIW2 priors are the worst performers, as they only identify two clusters for both data V and VI most of the time.

The sparse prior is the best performer overall. It recognizes 5 groups more often than all other priors for both settings. Adjusted Rand index values are consistently 1 for datasets V, as the model identifies true clusters perfectly, with three exceptions when it combined clusters. For the simulated data VI, adjusted Rand indices become more volatile, however, values are higher than those from the other priors on average.

Table 5
Information of the simulated data V with J=20. rep(a,b) represents a vector of length b with repeated elements a.

Cluster	μ_c^{true}	Var_c^{true}	ρ_c^{true}	n_c
1	(rep(3,5), rep(12,5), rep(18,5), rep(12,5))	3	0.7	200
2	(rep(12,5), rep(18,5), rep(3,5), rep(18,5))	3	0.7	200
3	(rep(18,5), rep(18,5), rep(12,5), rep(8,5))	3	0.7	200
4	(rep(18,5), rep(3,5), rep(8,5), rep(3,5))	3	0.7	200
5	(rep(8,5), rep(8,5), rep(12,5), rep(3,5))	3	0.7	200

Cluster No.	μ_c^{true}	$\operatorname{Var}_{c}^{true}$	$ ho_c^{true}$	n_c
1	(rep(3,5), rep(12,5), rep(18,5), rep(12,5))	9	0.7	200
2	(rep(12,5), rep(18,5), rep(3,5), rep(18,5))	9	0.7	200
3	(rep(18,5), rep(18,5), rep(12,5)rep(8,5))	9	0.7	200
4	(rep(18,5), rep(3,5), rep(8,5), rep(3,5))	9	0.7	200
5	(rep(8,5), rep(8,5), rep(12,5), rep(3,5))	9	0.7	200

When the clustering signal is strong, the separation prior also identifies 5 clusters quite often. However, its performance deteriorates greatly for a weaker signal. Adjusted Rand indices exhibit more variability than the sparse prior, as it combines true clusters more often. The HIW1 prior is not performing as well as the separation prior when the signal is relatively strong. When the signal becomes weak, however, it outperforms the separation prior. Finally, the independent prior again splits true clusters, which results in more groups identified in the final clustering.

Inferences on computational speed and posterior distributions for α are shown in the Supplemental material, Section S9, as they are similar to those in the previous subsection. Note that stability regarding the posteriors of α is not sufficient to indicate whether the DPMM generates sensible and stable partition results.

Further checks on the convergence of the MCMC chains were made. Two simulated datasets were randomly selected, one from data III and one from data V. We obtained trace plots for the adjusted Rand index, number of clusters and α , after running 6 MCMC chains with different initialisations. We also considered the posterior similarity matrices resulting from the different initialisations. For both data sets, the diagnostic plots indicated very good convergence for the Separation and Sparse priors, noting that the trace plot for the number of clusters under the Separation prior (data V) showed stickiness at 4 or 5 clusters. The diagnostic plots indicated that convergence was a problem under the other priors, with the HIW1 performing better compared to the HIW2, IW, Independent and Log priors. The fact that convergence was best achieved when the Separation and Sparse priors were used demonstrates that the choice of prior may not only improve on the modelling, but also on the convergence of the corresponding MCMC sampler, especially for challenging datasets such as the ones we simulated. Although the choice of prior appears to be crucial for achieving convergence and valid clustering outcomes, a different type of sampler (e.g a marginal sampler with split/merge steps) may be a plausible additional tool for addressing the problems described in Section 1. This investigation is beyond the scope of this manuscript. Output from the convergence checks for one dataset is included in Section S9 in the Supplemental material.

5. The role of sample size and initial values

Sample size is particularly important for generating sensible clustering results with mixture modelling, especially when the signal in the data is less strong. Sample size can be viewed as large or small after considering the cluster sizes n_c in relation to the number of parameters to be estimated.

Consider the previously specified data VI, but with an increased sample size of $n_c = 500$. We refer to this new specification as data VII. In Section S10 in the Supplemental material we display bar plots of the number of clusters identified by different priors. We also present boxplots of the adjusted Rand indices for different priors. Except for the independent prior, the tendency to

combine true clusters is alleviated for all priors. True clusters are identified more frequently, which translates to higher adjusted Rand indices. For the sparse prior, it can be observed that the adjusted Rand indices are always close to one, which is similar to the case when the signal is strong in simulated data V. Therefore, empirically, with a larger sample size, the resulting partitioning improves significantly. Note that, for the sparse prior, even with a sample size of 500 per cluster, the clustering results sometimes contain small clusters consisting of one or two subjects. This may be due to the tendency of the DPMM to create extra small clusters; see Miller and Harrison (2014) and Miller and Harrison (2017) for more details. As the conditional independence assumption does not hold, the independent prior identifies even more clusters when the sample size increases and adjusted Rand indices are lower than those for the simulated data VI.

Starting clustering allocation values for the DPMM sampler are also important. (This is true for other numerical approaches too, such as the EM algorithm; see Fraley and Raftery (2007).) Typically, there is a discrepancy between the overall covariance matrix and the within-cluster covariance matrices. When the DPMM is randomly initialized in terms of cluster allocation, the starting values of Σ_c will be similar to the overall covariance matrix. Then, when the signal is not strong, or the sample size is relatively small, clustering results can be unstable. One remedy is to generate more non-empty clusters than expected when randomly initializing the algorithm, as suggested by Hastie et al. (2015). One could also initialize the DPMM using some distance-based approach. For instance, one may use k-means, one of the proposed approaches in Celeux et al. (2018) where the initialization of the sampler for the sparse finite mixture model for large J is discussed. Such approaches usually require to set a fixed number of clusters. Since the goal is to make the starting values of Σ_c smaller, one can set the number of clusters to be much larger than the maximum number of clusters expected in the data. Starting values for Σ_c are then more likely to be reasonable. Based on our experience when using this approach to initialize the DPMM sampler, the clustering results can indeed be more stable most of the time. However, when the distance-based approach is not suitable given the shape of the clusters or the nature of the problem in general, this will reduce its effectiveness. Celeux et al. (2018) observed lack of mixing when initializing using k-means in high-dimensionality, and proposed to set the prior expected withincluster variances and covariances to be larger as J increases. This suggests that different initialization approaches can be relevant to specifying hyperparameter values for the prior of covariance matrices.

For the analyses in this manuscript we have not used a distance-based approach to derive starting values, as we wanted to focus purely on the comparative performance of the prior specifications under standard random initialisation.

6. Analysis of a real dataset

To further assess the priors' performance a real data set is analysed where true labels are known. The dataset is taken from the UCI Machine Learning Repository and is part of the RNA-Seq PAN-cancer dataset. The dataset contains 20,531 covariates and 801 subjects. Covariates contain gene expression measurements from patients with five distinct types of tumors, BRCA, KIRC, COAD, LUAD and PRAD. The cancer labels form the benchmark partition for this analysis. Since the number of covariates J is much larger than the number of subjects n, it is necessary to pre-select genes. All genes with zero observations were removed, reducing their number to 12,356. Genes with strong associations with the labels were selected, to effect a relatively strong clustering signals. Welch's t-test was adopted as it is robust under skewed distributions (Fagerland, 2012; Fagerland and Sandvik, 2009). Boxplots of resulting p-values are shown in the Supplemental material, Section S11. We selected the 20 genes with the smallest corresponding p-values. The Shapiro-Wilk test for Normality (p-values are shown in the Supplemental material Section S11) indicated that the observations are not normally distributed. This allows to draw inferences on the behaviour of the different priors when the normality assumption is not satisfied.

The overall covariance matrix and the benchmark partition are displayed in Figure 11. The first three principle components are used to visualise the data, as they explain 78% of the total variability. We run the sampler repeatedly for 30 different starting points for each prior, to assess stability, for a burn-in period of 10,000 iterations, followed by 6,000 iterations. The induced partitions were stable after the burn-in. Figure 12 shows the number of final clusters recognized for each prior given the different initialisations. As the variables are not normally distributed, the number of final clusters identified is usually larger than the benchmark and less stable compared to the simulated data analyses.

Figures 13 and 14 demonstrate that the clustering of the subjects may be notably different from the benchmark, even when the number of clusters identified is the same as the target number. On the other hand, the clustering of the subjects may be close to the benchmark when superfluous clusters are small. The log prior frequently recognizes a number of superfluous clusters that is larger compared to other priors. It also combines target clusters. Representative clusters for the log prior are not shown, as it is the worst performer in terms of adjusted Rand index. Figure 15 (left) displays boxplots of the adjusted Rand indices observed for each prior. Table 7 provides means and standard deviations of the adjusted Rand indices.

The independent prior always recognizes more clusters, as in the simulation studies. True clusters are split, not only for observations at the boundaries of the benchmark clusters, as shown in Figure 14. In terms of Rand index performance, it is only better than the log prior.

The separation prior generates superfluous clusters too, importantly some not small. Its Rand index performance is not satisfactory compared to other priors. Figure 14 shows an example of 12 final clusters from the separation prior.

The performance of the IW is also not satisfactory, as target clusters are often merged. With the HIW1 and HIW2 priors this problem alleviates, and their performance in terms of Rand index is good, only bettered by the sparse prior. However, small clusters are created at the boundaries of the benchmark

groups, and representative partitions are unstable for different initializations in terms of the final number of identified clusters. Figure 13 shows representative clustering examples of the 9 and 12 final clusters resulted from the HIW1. The partitions with the 9 and 12 final clusters are very similar. The difference lies in the small clusters created at the boundaries. Figure 13 displays clustering examples of the 8 and 10 final clusters resulted from the HIW2.

The number of clusters identified by the sparse prior is quite stable. The model frequently identifies 9 groups with no target clusters combined. Figure 14 shows one representative clustering of 9 final clusters. The superfluous clusters mostly exist at the boundaries of target clusters. The sparse prior outperforms all others, with the highest median adjusted Rand index and little variability.

Table 7
The mean and standard deviation of the Rand index of different priors

Prior type	mean of the adjusted Rand index	standard deviation of the adjusted Rand index
IW	0.771	0.098
HIW1	0.805	0.056
HIW2	0.816	0.059
Separation prior	0.740	0.062
Log prior	0.469	0.146
Sparse prior	0.841	0.002
Independent prior	0.609	0.097

Figure 15 (right) shows boxplots of run-times from the 30 initializations for different priors. Similar to the simulation studies, the log and separation priors are much slower than the rest. The sparse prior is not as quick as the IW, HIW1, HIW2 and independent priors, however, the disparity is relatively small. Information on the posterior distributions of α is given in the Supplemental material, Section S11.

7. Discussion

This manuscript provided a thorough overview and comparative investigation into possible priors for covariance matrices within the DPMM context, with detailed guidelines for their implementation, as done within the R package PRe-MiuM. In addition to investigating the effectiveness of different prior specifications, our aim was to make it easier for investigators to avoid, if desired, some of the standard approaches to fitting mixture models to high-dimensional data such as assuming diagonal covariance matrices; see, for instance, Banfield and Raftery (1993) or Galimberti and Soffritti (2013).

The sparse prior performed well in the different analyses, with the resulting partitions close to the target and stable. Our understanding is that to attain better clustering results, the prior of the within-cluster covariance matrices should be rather informative. Otherwise, it is difficult for both model and sampler to identify target clusters. Unlike classification problems where the latent labels are observed for part of the dataset, in unsupervised clustering there is no information on the underlying groups. If the sampled variances for the within-cluster

covariance matrices are larger than the truth, it is likely that target clusters are combined. The tuning of M_0 can be viewed as the process of setting a suitable prior for Σ_c using the structure of the observations. Note that for the HIW1, HIW2, separation and log priors, we also specify them to be rather informative in the sense that the prior mean variances in Σ_c are relatively small. This is an acceptable practice within the Bayesian paradigm, where the structure of the data can be used to inform the prior, rather than the individual observations themselves. In Richardson and Green (1997) for instance, weak informative priors are proposed, and it is pointed out that the possible spread of the clusters should be reflected in the prior. Sensitivity analyses we performed have shown that clustering results are not detached from the adopted hyperparameter values. This is a mixture modelling characteristic also mentioned by Celeux et al. (2018). In general, it is possible to improve clustering results by fine-tuning the specified hyperparameters to the specific application and dataset under consideration. Further research can be done towards a more systematic process for tuning M_0 , or the hyperparameters for the Separation, HIW1 and HIW2 priors, beyond the guidelines provided in this manuscript.

We focus on datasets where the number of variables J is beyond a handful (say 2 to 5), with unconstrained within-cluster covariance matrices Σ_c . In our manuscript, J is not of very large size, say 100 or 1000. Letting K denote the number of clusters or non-empty components in the mixture likelihood, Chandra et al. (2020) proved that as J approaches infinity with a fixed number of subjects, the probability of K=1 (all subjects belong to the same group) or K=n (each subject forms its own cluster) tends to one a posteriori. For datasets with very large J or even with $J\gg n$, Chandra et al. (2020) advocated to conduct factor analysis on the observed data. Clustering can then be applied to the derived factors. Therefore, results in this manuscript can also be useful for such high-dimensional problems, through the clustering of factors.

Although this manuscript focuses on the conditional samplers of the DPMM, it is also possible to incorporate the studied priors in marginal samplers with similar computational steps given in the Supplemental material, for example, Neal's Algorithm 8 (Neal, 2000). It may also be of interest to examine the possibility of including the split and merge step (Jain et al., 2007) in the marginal samplers for some of the priors mentioned in Section 2.

It is likely the DPMM creates extra small clusters that contain only a few subjects; see Miller and Harrison (2014). In light of this, Miller and Harrison (2017) advocated to use finite mixture models with a prior on the number of components, referred to as the mixture of finite mixtures (MFM), and designed a marginal sampler for the MFM based on the Algorithm 3 of Neal Neal (2000). Later, Frühwirth-Schnatter et al. (2020) extended results by Miller and Harrison (2017) and proposed the telescoping sampler for the MFM, which shares similarities with the conditional samplers for the DPMM. It should be possible to incorporate the sparse prior into the MFM using the telescoping sampler with similar steps discussed in the Supplemental material. This is currently under investigation.

Malsiner-Walli et al. (2016) proposed the sparse finite mixture model. The

main idea is to specify a finite mixture model with a maximum number of components much larger than the expected number of groups in the data. Then, a sparse prior is placed on the mixture weight $\Psi = \{\psi_1,, \psi_K\}$ to empty superfluous components. Malsiner-Walli et al. (2017) stated that the sparse finite mixture model is more suitable for scenarios where the data contain a moderate number of groups and the group number does not increase when more subjects are observed, whereas the DPMM can be more appropriately applied in scenarios where the number of clusters in the data increases with sample size, such as the text mining context. However, a strong correspondence does exist between the sparse finite mixture model and the DPMM. (See Frühwirth-Schnatter and Malsiner-Walli (2019) for a more detailed discussion). We currently investigate the possibility of incorporating the priors for Σ_c listed in Section 2 to the sparse finite mixture model and study how they can influence clustering outcomes.

In the real data analysis, we compared the clustering results with the clustering implied by the cancer labels. As we selected genes with expression highly associated with the tumor labels, it was reasonable to expect that the clustering results should closely match the benchmark clustering according to cancer type. To further encourage the clustering of the subjects to be similar to the tumor labels, we could have utilised a profile regression model, as in Molitor et al. (2010), also implemented within the PReMiuM R package, with tumor labels modelled as an outcome. However, to achieve a clean comparison between the priors, we decided against directly influencing the clustering of the subjects by including the tumor labels in the modelling. Finally, to identify genes that are important for the clustering, from a larger pool of genes than the 20 we selected, we could have utilised the variable selection approach implemented in PReMiuM Papathomas et al. (2012). However, variable selection is not the focus of this manuscript.

Bibliography

Banerjee, S. and Ghosal, S. (2013). "Bayesian estimation of a sparse precision matrix." arXiv preprint arXiv:1309.1754. 9

Banfield, D., Jeffrey and Raftery, A. E. (1993). "Model based Gaussian and Non-Gaussian clustering." *Biometrics*, 49: 803–821. 19

Barnard, J., McCulloch, R., and Meng, X.-L. (2000). "Modeling covariance matrices in terms of standard deviations and correlations, with application to shrinkage." *Statistica Sinica*, 1281–1311. 7

Blackwell, D. (1973). "Discreteness of Ferguson Selections." The Annals of Statistics, 1(2): 356–358. 3

Celeux, G., Kamary, K., Malsiner-Walli, G., Marin, J.-M., and Robert, C. P. (2018). "Computational Solutions for Bayesian Inference in Mixture Models."
In Frühwirth-Schnatter, S., Celeux, G., and Robert, C. P. (eds.), Handbook of Mixture Analysis, 77–100. Chapman and Hall/CRC. 5, 17, 20

Chandra, N. K., Canale, A., and Dunson, D. B. (2020). "Escaping the curse of dimensionality in Bayesian model based clustering." arXiv preprint arXiv:2006.02700. 2, 20

- Fagerland, M. W. (2012). "t-tests, non-parametric tests, and large studies: a paradox of statistical practice?" *BMC medical research methodology*, 12(1): 1–7. 18
- Fagerland, M. W. and Sandvik, L. (2009). "Performance of five two-sample location tests for skewed distributions with unequal variances." Contemporary Clinical Trials, 30(5): 490–496. 18
- Fan, J., Feng, Y., and Wu, Y. (2009). "Network exploration via the adaptive LASSO and SCAD penalties." The Annals of Applied Statistics, 3(2): 521. 9
- Fraley, C. and Raftery, A. E. (2007). "Bayesian regularization for normal mixture estimation and model-based clustering." *Journal of Classification*, 24(2): 155–181. 17
- Friedman, J., Hastie, T., and Tibshirani, R. (2008). "Sparse inverse covariance estimation with the graphical lasso." *Biostatistics*, 9(3): 432–441. 9
- Frühwirth-Schnatter, S. and Malsiner-Walli, G. (2019). "From here to infinity: sparse finite versus Dirichlet process mixtures in model-based clustering." Advances in Data Analysis and Classification, 13(1): 33–64. 21
- Frühwirth-Schnatter, S., Malsiner-Walli, G., and Grün, B. (2020). "Generalized mixtures of finite mixtures and telescoping sampling." arXiv preprint arXiv:2005.09918. 20
- Galimberti, G. and Soffritti, G. (2013). "Using conditional independence for parsimonious model-based Gaussian clustering." Statistics and Computing, 23: 625–638. 19
- Gelman, A. (2006). "Prior distributions for variance parameters in hierarchical models (comment on article by Browne and Draper)." Bayesian Analysis, 1(3): 515–534. 3
- George, E. I. and McCulloch, R. E. (1993). "Variable Selection via Gibbs Sampling." Journal of the American Statistical Association, 88(423): 881–889.
- (1997). "Approaches for Bayesian variable selection." *Statistica Sinica*, 339–373. 9
- Görür, D. and Rasmussen, C. E. (2010). "Dirichlet Process Gaussian Mixture Models: Choice of the Base Distribution." *Journal of Computer Science and Technology*, 25(4): 653–664. 6
- Hastie, D. I., Liverani, S., and Richardson, S. (2015). "Sampling from Dirichlet process mixture models with unknown concentration parameter: mixing issues in large data implementations." *Statistics and Computing*, 25(5): 1023–1037. 17
- Hennig, C., Meila, M., Murtagh, F., and Rocci, R. (2015). *Handbook of Cluster Analysis*. CRC Press. 4
- Huang, A. and Wand, M. P. (2013). "Simple Marginally Noninformative Prior Distributions for Covariance Matrices." *Bayesian Analysis*, 8(2): 439–452. 6
- Hubert, L. and Arabie, P. (1985). "Comparing partitions." Journal of Classification, 2(1): 193–218. 12
- Jain, S., Neal, R. M., et al. (2007). "Splitting and merging components of a nonconjugate Dirichlet process mixture model." *Bayesian Analysis*, 2(3): 445–472. 20

- Jara, A., Hanson, T. E., Quintana, F. A., Müller, P., and Rosner, G. L. (2011).
 "DPpackage: Bayesian Semi-and Nonparametric Modeling in R." Journal of Statistical Software, 40(5): 1. 4
- Khondker, Z. S., Zhu, H., Chu, H., Lin, W., and Ibrahim, J. G. (2013). "The Bayesian Covariance Lasso." Statistics and its Interface, 6(2): 243. 9
- Leonard, T. and Hsu, J. S. (1992). "Bayesian inference for a covariance matrix." The Annals of Statistics, 20(4): 1669–1696. 8, 9
- Lewandowski, D., Kurowicka, D., and Joe, H. (2009). "Generating random correlation matrices based on vines and extended onion method." *Journal of Multivariate Analysis*, 100(9): 1989–2001.
- Liverani, S., Hastie, D. I., Azizi, L., Papathomas, M., and Richardson, S. (2015). "PReMiuM: An R package for profile regression mixture models using Dirichlet processes." *Journal of Statistical Software*, 64(7): 1. 4, 5
- Lo, A. Y. (1984). "On a Class of Bayesian Nonparametric Estimates: I. Density Estimates." The Annals of Statistics, 351–357.
- Malsiner-Walli, G., Frühwirth-Schnatter, S., and Grün, B. (2016). "Model-based clustering based on sparse finite Gaussian mixtures." *Statistics and Computing*, 26(1-2): 303–324. 5, 20
- (2017). "Identifying mixtures of mixtures using Bayesian estimation." Journal of Computational and Graphical Statistics, 26(2): 285–295. 21
- Miller, J. W. and Harrison, M. T. (2014). "Inconsistency of Pitman-Yor process mixtures for the number of components." *The Journal of Machine Learning Research*, 15(1): 3333–3370. 17, 20
- (2017). "Mixture models with a prior on the number of components." *Journal* of the American Statistical Association, 1–17. 17, 20
- Milligan, G. W. and Cooper, M. C. (1986). "A study of the comparability of external criteria for hierarchical cluster analysis." *Multivariate Behavioral Research*, 21(4): 441–458. 12
- Mitchell, T. J. and Beauchamp, J. J. (1988). "Bayesian variable selection in linear regression." *Journal of the American Statistical Association*, 83(404): 1023–1032. 9
- Molitor, J., Papathomas, M., Jerrett, M., and Richardson, S. (2010). "Bayesian profile regression with an application to the National Survey of Children's Health." *Biostatistics*, 11(3): 484–498. 4, 5, 13, 21
- Neal, R. M. (2000). "Markov chain sampling methods for Dirichlet process mixture models." *Journal of Computational and Graphical Statistics*, 9(2): 249–265. 20
- O'Hagan, A. (1994). Kendall's advanced theory of statistics, volume 2B: Bayesian Inference. Edward Arnold. 4
- O'Malley, A. J. and Zaslavsky, A. M. (2008). "Domain-level covariance analysis for multilevel survey data with structured nonresponse." *Journal of the American Statistical Association*, 103(484): 1405–1418. 7
- Papathomas, M., Molitor, J., Hoggart, C., Hastie, D., and Richardson, S. (2012). "Exploring data from genetic association studies using Bayesian variable selection and the Dirichlet process: application to searching for gene × gene patterns." Genetic Epidemiology, 36(6): 663–674. 21

- Richardson, S. and Green, P. J. (1997). "On Bayesian analysis of mixtures with an unknown number of components (with discussion)." *Journal of the Royal Statistical Society: Series B (Statistical Methodology)*, 59(4): 731–792. 7, 20
- Sethuraman, J. (1994). "A constructive definition of Dirichlet priors." Statistica Sinica, 639-650. 3
- Tokuda, T., Goodrich, B., Van Mechelen, I., Gelman, A., and Tuerlinckx, F. (2011). "Visualizing distributions of covariance matrices." *Columbia Univ.*, *New York, USA, Tech. Rep*, 18–18. 4
- Walker, S. G. (2007). "Sampling the Dirichlet mixture model with slices." Communications in Statistics, Simulation and Computation, 36(1): 45–54.
- Wang, H. (2012). "Bayesian graphical lasso models and efficient posterior computation." *Bayesian Analysis*, 7(4): 867–886. 9, 10, 11
- Yuan, M. and Lin, Y. (2007). "Model selection and estimation in the Gaussian graphical model." *Biometrika*, 94(1): 19–35. 9

Acknowledgments

The first author would like to acknowledge the support of the School of Mathematics and Statistics, as well as CREEM, at the University of St Andrews, and the University of St Andrews St Leonard's 7th Century Scholarship.

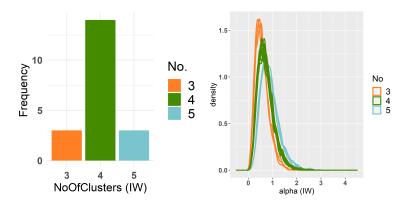


Fig 1. Bar plot of the estimated number of clusters (left) and the density of α (right) for simulated data I. The orange, green and blue colours correspond to 3, 4 or 5 estimated clusters respectively.

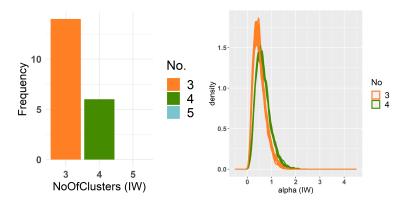


FIG 2. Bar plot of the estimated number of clusters (left) and the density of α (right) for simulated data II. The orange and green colours corresponds to 3 or 4 final clusters respectively in both plots.

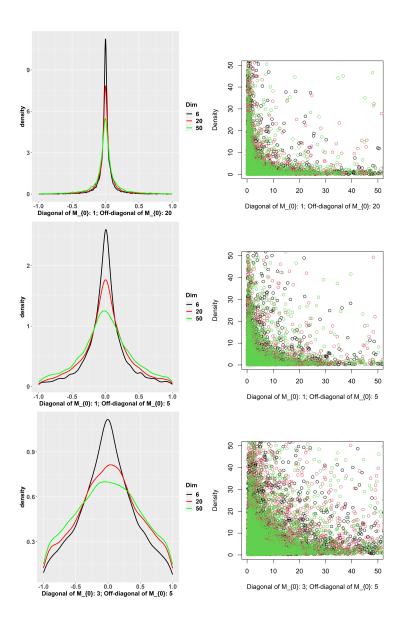


Fig 3. Empirical prior distributions of correlations when J=6, J=20 or J=50 for different M_0 (left). Empirical bivariate density plots of variances for J=6, J=20 or J=50 for different M_0 (right). The black colour corresponds to J=6; the red to J=20; the green to J=50. Diagonal of M_0 refers to $m_{0,ij}$.

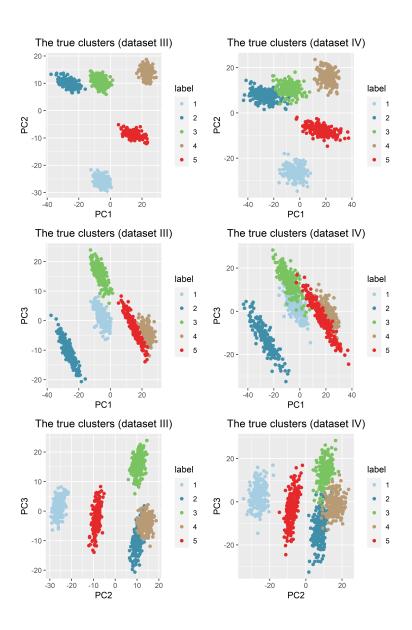


FIG 4. Reduced space plots of the clusters for simulated data III (Table 3) and IV (Table 4). A representative dataset is shown for each setting III and IV. PC1, PC3 and PC3 stand for the first, second and third principle component respectively.

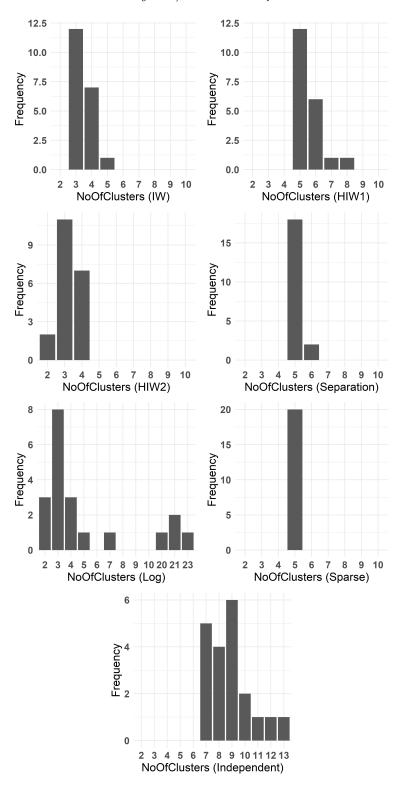


Fig 5. Bar plots of the number of clusters for the 20 datasets under set-up III (Table 3).

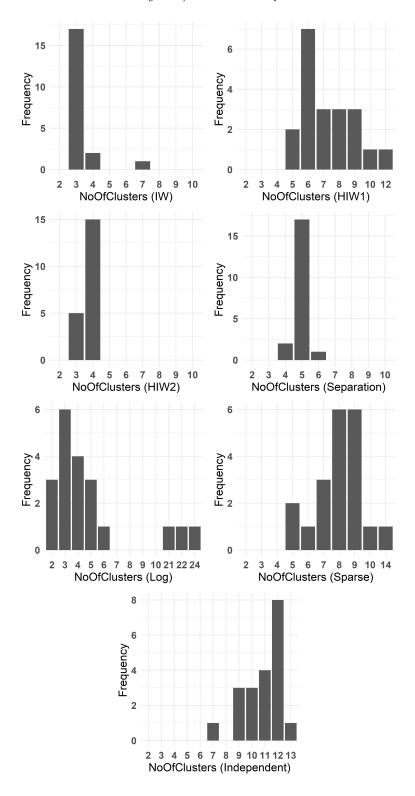


Fig 6. Bar plots of the number of clusters for the 20 datasets under set-up $IV\ (Table\ 4).$

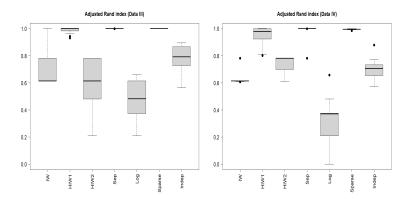


Fig 7. The boxplots of the adjusted Rand indices for different priors. The plot on the left corresponds to datasets simulated according to Table 3 (Data III). The plot on the right corresponds to datasets simulated according to Table 4 (Data IV).

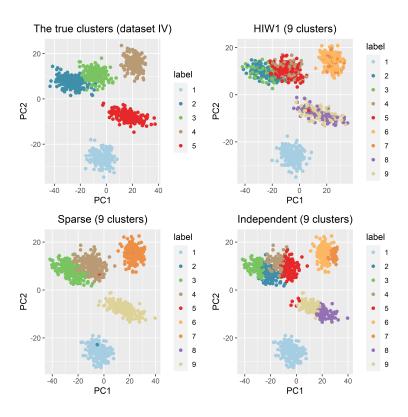


FIG 8. Reduced space plots of the true partition and one representative partition for the HIW1, sparse and independent priors for simulated data IV.

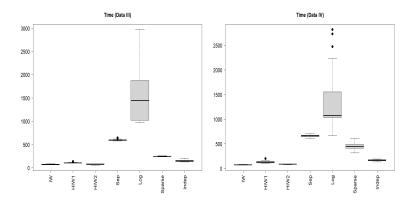


Fig 9. Computational time for the 20 datasets simulated according to Table 3 (Data III) on the left and Table 4 (Data IV) on the right in seconds.

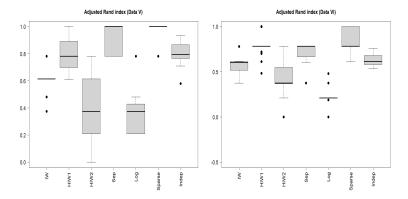


Fig 10. Boxplots of the adjusted Rand indices for different priors. The plot on the left corresponds to datasets simulated according to Table 5 (data V). The plot on the right corresponds to datasets simulated according to Table 6 (data VI).

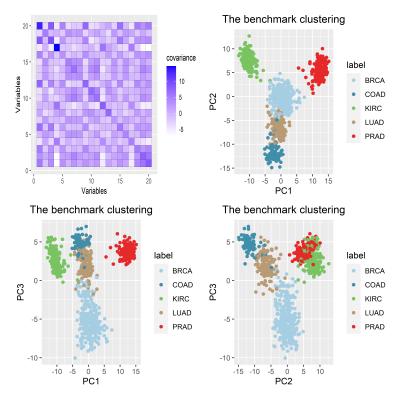


Fig 11. Overall correlation matrix of the 20 selected variables on the topleft. Remaining illustrations show reduced space plots of the benchmark clustering according to the cancer labels.

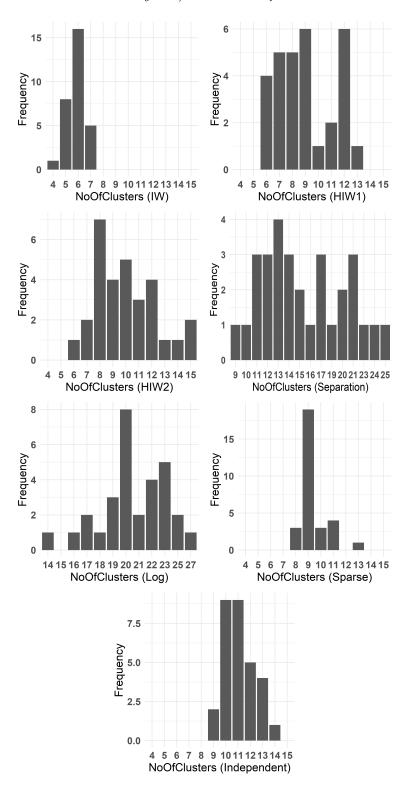


FIG 12. Bar plots of the number of identified clusters for 30 different initializations. The prior used is shown within the brackets in the x-axis label.

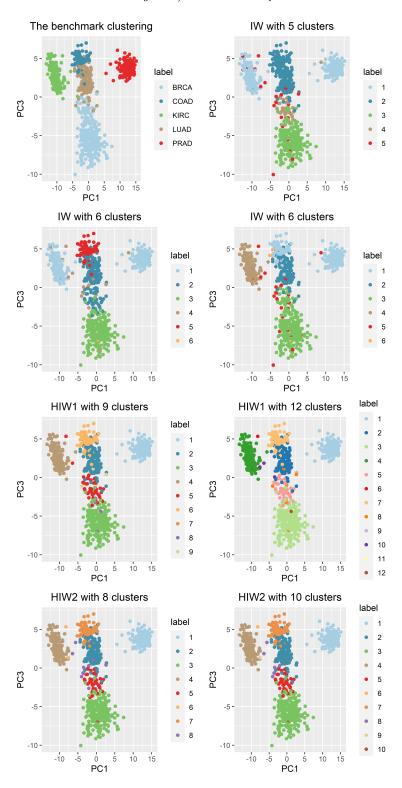


Fig 13. One representative clustering for a certain number of clusters for priors IW, HIW1 and HIW2.

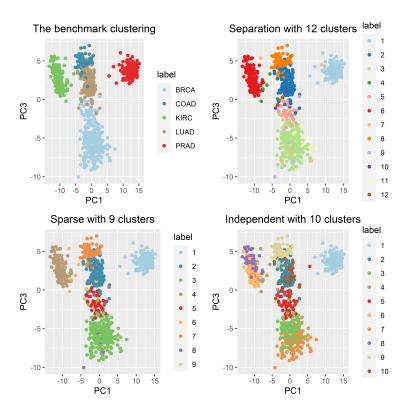


FIG 14. One representative clustering for a certain number of clusters for the separation, sparse and independent priors.

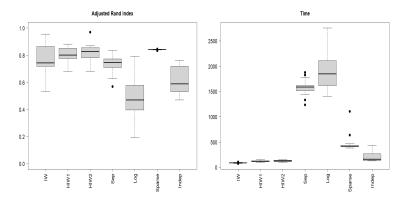


Fig 15. Boxplots of adjusted Rand indices for different priors (left) and computational times after running $30~{\rm seeds}$ (right) in seconds.